

Two-Dimensional O₂ Adsorbed on Graphite

R. D. Etters and Ru-Pin Pan

Physics Department, Colorado State University, Fort Collins, Colorado 80523

and

V. Chandrasekharan

Laboratoire des Interactions Moléculaires et Hautes Pressions, Centre National de la Recherche Scientifique, Université Paris-Nord, F-93430 Villetaneuse, France

(Received 23 June 1980)

Properties of two-dimensional O₂ adsorbed on graphite are calculated in the extremely low-coverage δ region and for monolayers, with use of pattern-recognition optimization and Monte Carlo techniques. Equilibrium configurations and orientations, orientational order-disorder, melting, and dissociation transitions are predicted at various O₂ densities. Phase characteristics, including a plastic crystallite phase, are compared with experiment.

PACS numbers: 68.60.+q, 67.80.Gd, 68.55.+b

Properties of two-dimensional (2D) oxygen physisorbed on graphite have been investigated with use of neutron diffraction,¹ low-energy electron diffraction,² and heat capacity measurements.³ From the data, a phase diagram has been partially mapped out¹ and is shown in Fig. 1. The solid lines outline the phase boundaries deduced from scattering data and the triangles give the δ -phase melting line at $\rho = 0.45$ and 0.3 from very recent specific-heat measurements.³ The number of O₂ molecules per unit area ρ is scaled so that the well-known $\sqrt{3} \times \sqrt{3}$ structure corresponds to unity. Monolayer coverage occurs at $\rho = 1.69$ and the 2D α and β phases are apparently structurally and orientationally characteristic of the densest packed planes of bulk α - and β -O₂, respectively. There is no evidence of a commensurate phase.¹

In the extreme δ phase where $\rho \ll 1$, calculations based upon the physics of infinite 2D layers are unable to provide an interpretation of the very

limited experimental data.^{1,4} As an alternative model for this regime we propose that small two-dimensional clusters of O₂ are formed and are distributed in size and space on the surface in a distribution that is dictated by substrate and cluster properties. An objective of this work is to investigate the thermodynamic properties of these clusters and to interpret the results in connection with our proposed model. To provide greater contact with experiment we have also calculated properties of the relatively data-rich infinite monolayer state.

The calculational methods we employ are a pattern-search optimization technique, and a Monte Carlo procedure, both of which are discussed in detail elsewhere.⁵ The O₂-O₂ potential is chosen to be the Lennard-Jones 6-12 atom-atom form of English and Venables,⁶ plus a quadrupole potential with moment $Q = -0.39 \times 10^{-26}$ esu cm². The parameters $(\sigma, \epsilon)_O = (3.05 \text{ \AA}, 54.335 \text{ K})$. The O₂-C potential is also taken to be of the 6-12 atom-atom form, where the parameters are chosen by the standard averaging procedure using $(\epsilon, \sigma)_C = (28 \text{ K}, 3.40 \text{ \AA})$ ⁷ for the carbon-carbon potential and the above mentioned parameters for O₂-O₂. The total substrate-O₂ interaction is calculated with use of the expansion of Steele,⁷ truncated after the second term. We neglect the magnetic interaction because the exchange energy is poorly understood^{1,8} and because estimates of the nearest-neighbor magnetic coupling constant indicate that it is less than⁸ 2% of that given by the O₂-O₂ potential. Thus, our studies are more appropriate for the paramagnetic β phase and the extreme δ phase.

For monolayer coverages of O₂ on graphite we

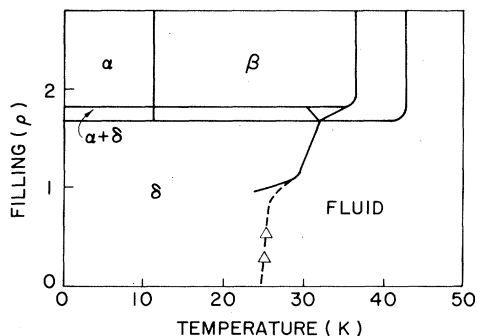


FIG. 1. Phase diagram for O₂ adsorbed on Grafoil. The α , β , and δ phases are solid and the lines refer to phase boundaries.

have carried out an optimization program with periodic boundary conditions assuming a two-sublattice model. Because of the uncertain accuracy of our O_2 -C potential, we have calculated system properties using the full anisotropic potential and separately with a spherically symmetric representation of the O_2 -C potential. The dashed line in Fig. 2 gives the total interaction energy per unit surface area, where the O_2 -C interaction has been spherically averaged. The energy minimum occurs for an unregistered equilateral-triangle lattice with a nearest-neighbor distance $d = 3.18 \text{ \AA}$, and the O_2 molecular axes are perpendicular to the surface. These results are in agreement with neutron scattering data¹ for the β phase although d departs from the experimental value of 3.28 \AA by about 3%. The adsorption energy, which we define as the total interaction energy of the O_2 with the substrate, is $-4.9 (4\epsilon)$. Results obtained with use of the anisotropic O_2 -C atom-atom potential are represented by the solid line on Fig. 2. The total interaction energy per unit area (E_T/A) is a minimum at $\rho \approx 1.8$. Moreover, the O_2 molecules sit on an unregistered equilateral-triangular lattice with their molecular axes perpendicular to the surface plane. These results are virtually identical to

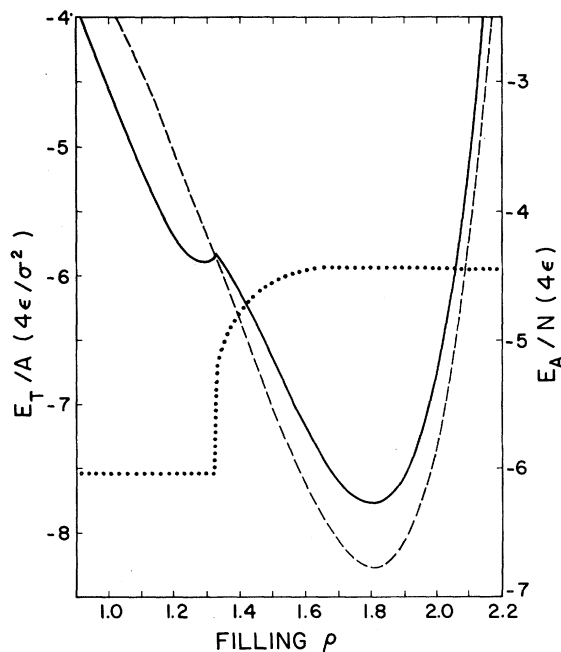


FIG. 2. Total interaction energy per unit surface area of O_2 on Grafoil vs coverage (left-hand scale) and adsorption energy (right-hand scale).

the case where the O_2 -C potential was sphericalized. However, a sharp change in E_T/A occurs at $\rho \approx 1.33$, accompanied by an orientational transition where the O_2 molecular axes become parallel to the substrate plane and to one another. The lattice is distorted into isosceles triangles with O_2 molecules at each vertex pointing along the perpendicular bisector. The sides of the triangle are 3.17 and 4.99 \AA . The dotted line gives the total adsorption energy per O_2 molecule (right-hand scale) for this case. The local minimum in E_T/A at $\rho \approx 1.29$ is actually the absolute minimum in E_T/N , where N is the number of O_2 molecules on the surface.

As a part of our model of the extreme δ region $\rho \ll 1$, we have investigated the thermodynamic properties of two-dimensional clusters of size $2 \leq N \leq 12$. Based upon the spherically symmetric C- O_2 potential, Fig. 3 shows the expectation value of the internal energy per O_2 molecule versus temperature, for $N = 7$. From $0 \leq T \leq 11 \text{ K}$, the O_2 molecules form a perfect hexagon with one in the middle, and their molecular axes are perpendicular to the substrate plane. With increasing temperature, the molecular fluctuations about this orientation increase until at $T = 11 \text{ K}$, an abrupt orientational order-disorder transition takes place into a hindered-rotor, plastic crystallite phase. This is evidenced by an abrupt change in the slope of the energy-temperature curve (Fig. 3) and by an abrupt change in the orientational order parameter which, in this case,

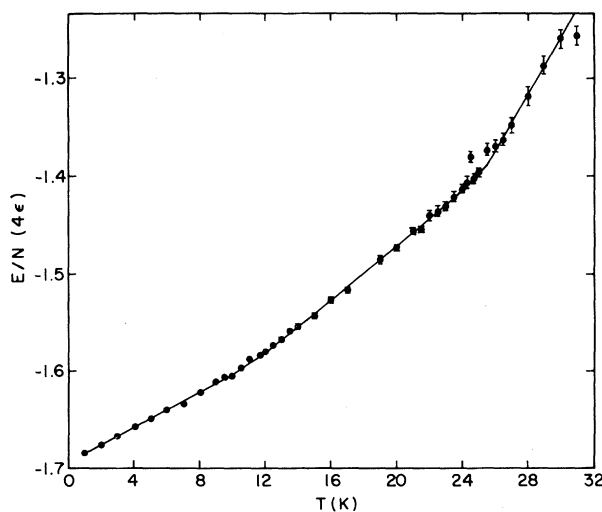


FIG. 3. Expectation value of the internal energy vs temperature for $N = 7$. Flags represent the statistical uncertainty.

is just the thermodynamic expectation value of $|\cos\theta_{ij}|$, where θ_{ij} is the angle between axes of molecules i, j . This quantity is given in Fig. 4. The two different curves correspond to the two inequivalent bonds for $N=7$. From $11 \leq T \leq 25$ K the cluster is in a plastic crystallite phase (translationally ordered but orientationally disordered). At $T=25$ K, another sharp break occurs in the energy, signaling a melting transition. As with the orientational transition, there are a number of tests that identify the character of the melting transition. One of these is the expectation value of the rms bond-length fluctuations between O_2 molecules, which sharply increases at $T=25$ K. Other evidence⁹ leads to the same conclusion. As the temperature rises to 38 K, the cluster dissociates into monomers constrained to a 2D plane. All cluster sizes exhibit the same qualitative behavior.

Table I gives calculated results for various cluster sizes and for the infinite film where T_O , T_M , T_D , d , and $E_0/4N\epsilon$ are the orientational order-disorder transition temperature, melting temperature, dissociation temperature, nearest-neighbor separation, and the interaction energy per O_2 molecule at 1.0 K, excluding the adsorption energy. Clusters with more than one orientationally inequivalent site may have more than one value for T_O .

Shapes are determined by the expectation value of the O_2 positions, which are at points of maximum coordination number. Thus, the equilibrium configurations for $N < 6$ are uniquely specified. Isomeric states first appear for $N=6$ and the ground state forms an incomplete hexagon. $N=7$ forms a hexagon and $N=12$ is formed from three interpenetrating hexagons. It is likely that larger

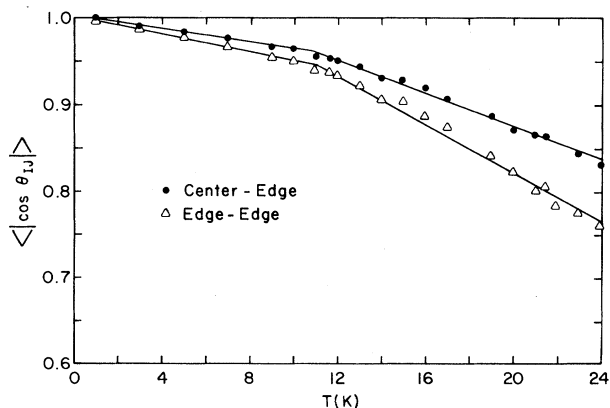


FIG. 4. Orientational order parameter for $N=7$ vs temperature.

clusters also grow by the formation of interpenetrating hexagons, much like the icosahedral formation in 3D rare-gas crystallites.⁵ In all cases O_2 axes are perpendicular to the substrate plane. The increase with increasing N of T_O , T_M , T_D , and E_0 can be attributed to the approach toward saturation of the bonds as N increases.

Several of the cluster results seem to agree with experimental evidence.¹⁻⁴ For example, the nearest-neighbor separations (Table I) are very near those values predicted from δ -phase neutron scattering data and the equilateral triangular structures and O_2 orientations are also consistent with that data. Another example is the δ -phase melting line which has been mapped down to $\rho \approx 1$ by neutron scattering¹ and also at $\rho = 0.3$ and 0.45 by specific heat measurements³ (see Fig. 1). A reasonable extrapolation of that data to $\rho \ll 1$, dashed line in Fig. 1, indicates that melting may occur near 25 K. Our work gives $18 \leq T_M \leq 29 \pm 2$ K for $N \leq 12$ and, because the O_2 binding energy for $N=12$ is nearly saturated (approaching monolayer values; see Table I), T_M will not increase much even for much larger clusters. Thus, the cluster results seem to be in reasonable agreement with the extrapolation of experimental melting data. Another interesting result is that molecules interior to the cluster edge do not undergo rotational transitions prior to melting but all edge molecules do. This leads us to speculate that edge molecules in a monolayer undergo rotational transitions prior to melting

TABLE I. Calculated properties of O_2 clusters. (See text for a discussion on values enclosed in parentheses.)

N	T_O (K)	T_M (K)	T_D (K)	d (Å)	$-E_0/4N\epsilon$
2			23	3.36 (3.39)	0.49
3	5.0 ± 0.5		26 (22)	3.36 (3.81)	0.94
4	5.1 ± 0.5 10.5 ± 0.3	20 ± 1 (~16)	32 (~30)	3.35 (3.48)	1.19
5	5.5 ± 0.5 11 ± 0.5 14 ± 0.5	19 ± 1 (~16)	38 (~32)	3.36 (3.39)	1.35
6	7 ± 0.3 14 ± 0.3	18 ± 1 (~14)	39 (~32)	3.35 (3.39)	1.46
7	11 ± 0.5	25 ± 2 (~16)	40 (~35)	3.35 (3.39)	1.68
12	11 ± 0.4 15 ± 0.5	29 ± 2	40	3.34	2.01
∞		36-44		3.29	2.83

but interior ones do not.

The full O₂-C potential gives results qualitatively similar to those calculated with use of the spherically symmetric expression except that the O₂-C anisotropies cause the O₂ molecules to lie flat on the substrate and the triangular structure is distorted by the anisotropy. Some results for this case are given in parentheses in Table I. For $N \leq 6$, $T_O \approx 4$ K; and for $N = 7$, $T_O \approx 6$ K. In the plastic crystallite phase, $T_O \leq T < T_M$, the O₂ molecules relax from the distorted configurations to 2D structures constructed by connecting equilateral triangles. This is caused by the O₂ rotations averaging out the anisotropies responsible for the distortion. There is no indication of registry.

To summarize our work on infinite O₂ monolayers, it is significant that the nearest-neighbor separation agrees to within 3% of experiment and is almost exactly the same for those calculations on bulk β -O₂ that used the English-Venables potential.⁶ This, coupled with our determination of an equilateral-triangular lattice and O₂ orientations perpendicular to the substrate, supports the view that 2D monolayers have the same character as the densest, packed plane of bulk O₂. Depending on the strength of the O₂-C anisotropy, a possible new low-density state at $\rho \approx 1.29$ is also predicted, where the O₂ lay flat on the substrate.¹⁰

In the fractional-monolayer $\rho \ll 1$ region, our 2D-cluster model gives structures, nearest-neighbor distances, orientations, melting temperatures, etc., that are consistent with experi-

ment.^{1-4,10} Particularly unusual are the well-defined orientational order-disorder transitions into a plastic crystallite phase. Our results indicate that monolayer O₂ will gasify at $T \approx 55$ K.

This work was supported by the National Aeronautics and Space Administration under Contract No. NGR-06-002-159.

¹M. Nielsen and J. P. McTague, Phys. Rev. B **19**, 3096 (1979).

²M. D. Chinn and S. C. Fain, Phys. Rev. Lett. **39**, 146 (1977).

³R. Marx and R. Braun, Solid State Commun. **33**, 229 (1980).

⁴O. Vilches, unpublished.

⁵R. D. Eppers and Jaya Kaelberer, Phys. Rev. A **11**, 1068 (1975); R. P. Pan and R. D. Eppers, J. Chem. Phys. **72**, 1741 (1980).

⁶C. A. English and J. A. Venables, Proc. Roy. Soc. London, Ser. A **340**, 57 (1974).

⁷W. A. Steele, Surf. Sci. **36**, 317 (1973).

⁸C. A. English, J. A. Venables, and D. R. Salahub, Proc. Roy. Soc. London, Ser. A **340**, 81 (1974).

⁹R. D. Eppers and Jaya Kaelberer, J. Chem. Phys. **66**, 5112 (1977).

¹⁰We have just learned of heat capacity and x-ray scattering data, to be published by O. Vilches and by R. J. Birgeneau and P. Stephens, which agrees qualitatively and quantitatively with our predicted low-density "laying flat" state. This contradicts earlier experiments (Ref. 1). There is also new evidence that the δ -phase melting line approaches $\rho = 0$ at $T \approx 25$ K as we predict; see Fig. 1.

Structure of Amorphous Silicon and Silicon Hydrides

T. A. Postol, Charles M. Falco, R. T. Kampwirth, and Ivan K. Schuller
Solid State Science Division, Argonne National Laboratory, Argonne, Illinois 60439

and

W. B. Yelon

Research Reactor Facility and Physics Department, University of Missouri, Columbia, Missouri 65211
(Received 28 April 1980)

Neutron scattering measurements have been made on pure, hydrogenated, and deuterated samples of amorphous silicon (α -Si) in the wave-vector range 0.007 – 8.75 \AA^{-1} . Small-angle data indicate structures in the samples of average radius of gyration as large as 270 \AA . Large-angle data show that for the concentrations we have measured (14%), the structure of α -Si is not altered by the incorporation of large amounts of H or D. The silicon-hydrogen and silicon-deuterium partial structure factors have also been obtained.

PACS numbers: 61.40.Df, 61.12.Dw, 72.80.Ng

Amorphous silicon (α -Si) and hydrogenated α -Si have received considerable attention very recently.¹ This has been motivated by recent interest

in the general subject of amorphous materials as well as by the discovery that incorporation of hydrogen changes the conductivity of α -Si by sever-